

# The Coolest ‘Stars’ are Free-Floating Planets

V. Joergens<sup>1,2</sup>, M. Bonnefoy<sup>3</sup>, Y. Liu<sup>4</sup>, A. Bayo<sup>1</sup>, S. Wolf<sup>5</sup>

<sup>1</sup>*Max-Planck Institut für Astronomie, Königstuhl 17, 69117 Heidelberg, Germany*

<sup>2</sup>*Institut für Theoretische Astrophysik, Zentrum für Astronomie der Universität Heidelberg, Albert-Ueberle-Str. 2, 69120 Heidelberg, Germany*

<sup>3</sup>*Institut de Planétologie et d’Astrophysique de Grenoble, UMR 5274, Grenoble, 38041, France*

<sup>4</sup>*Purple Mountain Observatory & Key Laboratory for Radio Astronomy, Chinese Academy of Sciences, Nanjing 210008, China*

<sup>5</sup>*Institut für Theoretische Physik und Astrophysik, Universität Kiel, Leibnizstr. 15, 24118 Kiel, Germany*

**Abstract.** We show that the coolest known object that is probably formed in a star-like mode is a free-floating planet. We discovered recently that the free-floating planetary mass object OTS 44 (M9.5,  $\sim 12$  Jupiter masses, age  $\sim 2$  Myr) has significant accretion and a substantial disk. This demonstrates that the processes that characterize the canonical star-like mode of formation apply to isolated objects down to a few Jupiter masses. We detected in VLT/SINFONI spectra that OTS 44 has strong, broad, and variable Paschen  $\beta$  emission. This is the first evidence for active accretion of a free-floating planet. The object allows us to study accretion and disk physics at the extreme and can be seen as free-floating analog of accreting planets that orbit stars. Our analysis of OTS 44 shows that the mass-accretion rate decreases continuously from stars of several solar masses down to free-floating planets. We determined, furthermore, the disk mass (10 Earth masses) and further disk properties of OTS 44 through modeling its SED including Herschel far-IR data. We find that objects between 14 and 0.01 solar masses have the same ratio of the disk-to-central-mass of about 1%. Our results suggest that OTS 44 is formed like a star and that the increasing number of young free-floating planets and ultra-cool T and Y field dwarfs are the low-mass extension of the stellar population.

## 1. Introduction

We have witnessed in the last decade the detection of free-floating substellar objects with increasingly lower masses and cooler temperatures that reach the canonical planetary regime of a few Jupiter masses and a few hundred Kelvin. Examples are free-floating planetary mass objects in star-forming regions (e.g., [Zapatero Osorio et al. 2000](#)) and ultracool Y dwarfs in the field (e.g., [Cushing et al. 2011](#)). One of the main open questions in the theory of star formation is: How do these free-floating planetary-like objects - and brown dwarfs in general - form? A high-density phase is necessary for the gravitational fragmentation to create very small Jeans-unstable cores. Proposed scenarios to prevent a substellar core in a dense environment from accreting to stellar mass are ejection of the core through dynamical interactions (e.g., [Reipurth & Clarke 2001](#)) or photo-evaporation of the gas envelope through radiation of a nearby hot star (e.g., [Whitworth & Zinnecker 2004](#)). Also suggested was the formation of brown dwarfs by disk instabilities in the outer regions of massive circumstellar disks (e.g., [Stamatellos & Whitworth 2009](#)). Alternatively, brown dwarfs could form in a more isolated mode by direct collapse. For example, filament collapse (e.g., [Inutsuka & Miyama 1992](#)) might form low-mass cores that experience high self-erosion in outflows and become brown dwarfs ([Machida et al. 2009](#)). A key to understanding star and brown dwarf formation is to observationally define the minimum mass that the canonical star-like mode of formation can produce by detecting and exploring the main features characteristic of this process, such as disks, accretion, outflows, and orbiting planets, for the lowest-mass objects.

The first indications for the existence of free-floating planetary mass objects came from observations in the very young  $\sigma$  Orionis cluster ([Zapatero Osorio et al. 2000](#)). While it is difficult to establish the membership to  $\sigma$  Ori and, therefore, the age and mass, some very promising candidates were detected. An example is S Ori 60, for which mid-IR excess indicates a young age ([Luhman et al. 2008a](#)). Other candidates, however, turned out not to be members of the cluster, such as S Ori 70 ([Burgasser et al. 2004](#); Peña Ramirez, this volume). The coolest known free-floating objects are Y dwarfs, of which 17 are spectroscopically confirmed to date ([Cushing et al. 2014](#)). While we can expect many planetary mass objects among Y dwarfs, the age and mass of these nearby field objects are in most cases unknown. The first confirmed Y dwarf, WISE 1828+2650 ([Cushing et al. 2011](#)), was suggested to have a temperature and mass of only about 300 K and 3-6  $M_{\text{Jup}}$ , respectively, although there are indications that the temperature might be significantly larger ([Dupuy & Kraus 2013](#)). Very recently a remarkably cold and low-mass object was detected in the very near vicinity of our Sun: WISE 0855-0714 at a distance of 2.2 pc has a proposed temperature and mass of 250 K and 3-10  $M_{\text{Jup}}$ , respectively ([Luhman 2014](#)). Nearby objects that do allow constraints on their age and, therefore, mass are members of young moving groups (see also Faherty, this volume). One of them, PSO J318.5-22, was recently detected to be a planetary-mass member of  $\beta$  Pic. Depending on the assumed age for  $\beta$  Pic its mass is estimated to 6.5  $M_{\text{Jup}}$  (age: 12 Myr) and 8.4  $M_{\text{Jup}}$  (21 Myr), respectively ([Liu et al. 2013](#); Allers, this volume).

To address the question how free-floating planets form, we observed OTS 44, the lowest mass known member of the Chamaeleon I star-forming region (Cha I,  $\sim 2$  Myr, 160 pc). OTS 44 was first identified as a brown dwarf candidate in a deep near-IR imaging survey ([Oasa et al. 1999](#)) and later confirmed as very low-mass substellar object of spectral-type M9.5 based on low-resolution near-IR and optical spectra (e.g. [Luhman et al. 2004](#)). Its mass was estimated using near-IR spectra to lie in or very close to the planetary regime ( $\sim 6$ -17  $M_{\text{Jup}}$ , [Bonnetfoy et al. 2013](#)) with an average rounded value of 12  $M_{\text{Jup}}$ .

## 2. OTS 44 - a 12 Jupiter mass object with a substantial disk

Mid-IR photometry of OTS 44 by Spitzer/IRAC and MIPS (Luhman et al. 2008b) indicated the presence of circumstellar material surrounding OTS 44. Recently, the disk of OTS 44 was detected at far-IR wavelength by Herschel/PACS (Harvey et al. 2012). We re-analyzed the Herschel flux measurement (Joergens et al. 2014) and find a slightly smaller value for OTS 44 than Harvey et al. (2012).

We modeled the SED of OTS 44 based on flux measurements from the optical to the far-IR using the radiative transfer code MC3D (Wolf 2003). We employ a passive-disk model consisting of a central substellar source surrounded by a parameterized flared disk in which dust and gas are well mixed and homogeneous throughout the system. We assume dust grains of astronomical silicate (62.5%) and graphite (37.5%) with minimum and maximum grain sizes of  $0.005 \mu\text{m}$  and  $0.25 \mu\text{m}$ , respectively. As there are model degeneracies between different disk parameters, we conducted a Bayesian analysis to estimate the validity range for each parameter. See Joergens et al. (2013) for details. Fig. .1 shows the SED and the best-fit disk model of OTS 44 based on the re-analysis of the Herschel fluxes (Joergens et al. 2014). We find that OTS 44 has a highly flared disk ( $\beta > 1.3$ ) with a disk mass of  $3.25 \times 10^{-5} M_{\odot}$ , i.e. about  $10 M_{Earth}$ .

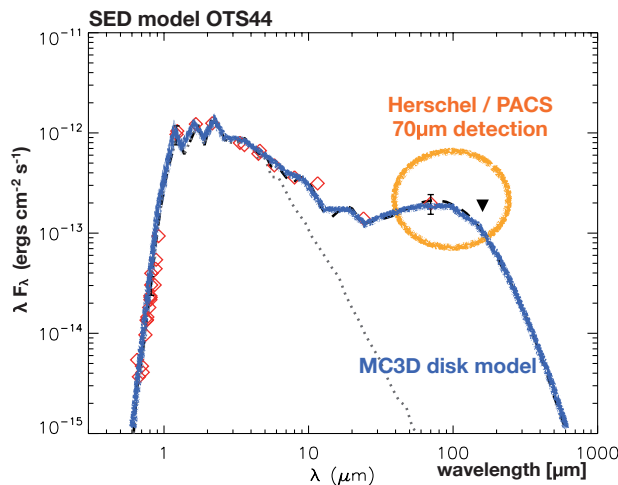


Figure .1: SED of OTS 44. Shown are photometric measurements (red diamonds) an upper limit for the  $160 \mu\text{m}$  flux (black triangle), the best-fit SED model (blue thick line), and the input BT-Settl photosphere model (gray dotted line). This is a slightly revised version of the SED model of OTS 44 in Joergens et al. (2013) using a revised Herschel flux measurement (Joergens et al. 2014).

## 3. OTS 44 - a 12 Jupiter mass object with significant accretion

We took near-IR J-band spectra ( $1.1\text{-}1.4 \mu\text{m}$ ) of OTS 44 with SINFONI at the VLT at a medium spectral resolution ( $R = \lambda / \Delta\lambda \sim 2000$ , Bonnefoy et al. 2013). We discovered a strong,

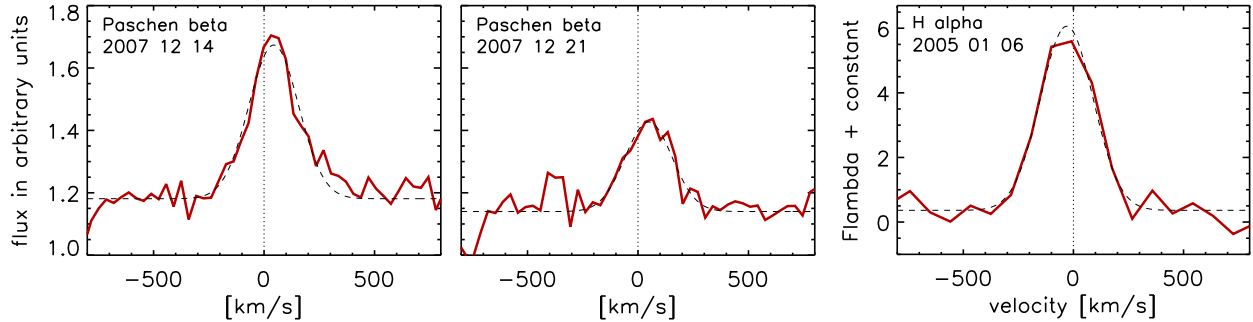


Figure .2: Pa  $\beta$  emission of OTS 44 in VLT/SINFONI spectra (left, middle) and H $\alpha$  emission of OTS 44 in a MAGELLANI/IMACS spectrum (right). The dashed lines are Gaussian fits to the profiles. From Joergens et al. (2013).

broad, and variable Paschen  $\beta$  (Pa  $\beta$ ) emission line of OTS 44 in these spectra (Joergens et al. 2013), as shown in Fig. .2 (left, middle). Furthermore, a prominent H $\alpha$  emission line is visible in the optical spectrum of Luhman (2007) as shown in the right panel of Fig. .2. Both of these Hydrogen emission lines exhibit a broad profile with velocities of  $\pm 200 \text{ km s}^{-1}$  or more. We determined the equivalent width (EW) of both lines. The H $\alpha$  line has a symmetrically shaped profile with an EW of  $-141 \text{ \AA}$ , demonstrating that OTS 44 is actively accreting. The profile of the Pa  $\beta$  line is significantly variable between the two observing epochs separated by a few days (EW of  $-7$  and  $-4 \text{ \AA}$ ).

We determined the mass accretion rate of OTS 44 based on the H $\alpha$  line by assuming that the H $\alpha$  emission is entirely formed by accretion processes. We derived an H $\alpha$  line luminosity  $\log L_{H\alpha} (L_{\odot})$  of  $-6.16$  for OTS 44 and applied the empirical relation between the H $\alpha$  line and accretion luminosity of Fang et al. (2009), which is based on  $\log L_{H\alpha} (L_{\odot})$  ranging between  $-1$  and  $-6$ . We estimate an mass accretion rate of OTS 44 of  $7.6 \times 10^{-12} M_{\odot} \text{ yr}^{-1}$ .

#### 4. Conclusions

We have discovered strong, broad, and variable Pa  $\beta$  emission of the young very low-mass substellar object OTS 44 (M9.5) in VLT/SINFONI spectra, which is evidence for active accretion of a planetary mass object (Joergens et al. 2013). We determined the properties of the disk that surrounds OTS 44 through MC3D radiative transfer modeling of flux measurements from the optical to the far-IR including Herschel data (Joergens et al. 2013, 2014). We found that OTS 44 has a highly flared disk ( $\beta > 1.3$ ) with a mass of  $3.25 \times 10^{-5} M_{\odot}$ , i.e. about  $10 M_{Earth}$ . We also investigated the H $\alpha$  line of OTS 44 in a MAGELLANI/IMACS spectrum and found strong H $\alpha$  emission with an EW of  $-141 \text{ \AA}$  indicative of active accretion. Both the Pa  $\beta$  and H $\alpha$  emission lines of OTS 44 have broad profiles with the wings extending to velocities of about  $\pm 200 \text{ km s}^{-1}$ . The Pa  $\beta$  emission is significantly variable on timescales of a few days, indicating variability in accretion-related processes of OTS 44. We estimated the mass accretion rate of OTS 44 to  $7.6 \times 10^{-12} \text{ yr}^{-1}$  by using the H $\alpha$  line. A mass accretion rate based on the Pa  $\beta$  line gives a significantly higher value, and we speculate that part of the Pa  $\beta$  emission might come from other processes related to accretion, such as outflows. Furthermore, in the course of studying OTS 44, we fitted a

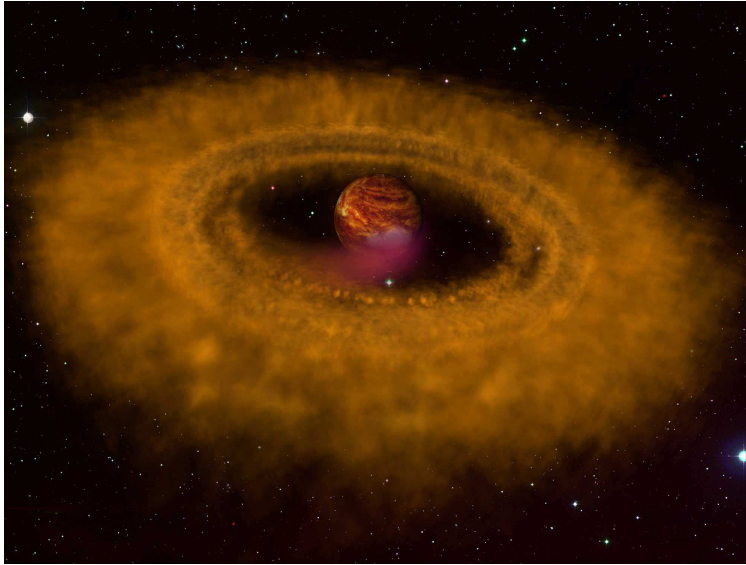


Figure .3: Artist's view of the accreting and disk-bearing free-floating planetary mass object OTS 44. Credit: MPIA / A. M. Quetz.

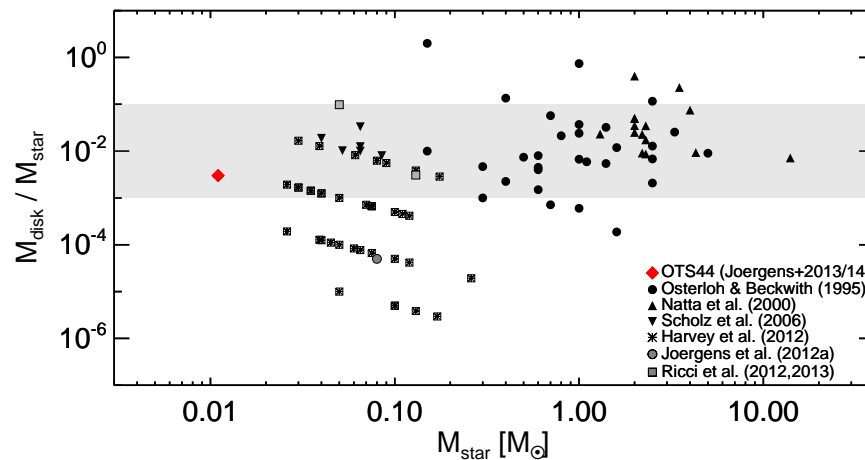


Figure .4: Relative disk mass versus central mass of stars and brown dwarfs including OTS 44 (red diamond). Slightly revised version of similar plot from Joergens et al. (2013).

photospheric BT-Settl model to its optical and near-IR SED and derived a lower effective temperature and higher extinction than was previously found (Luhman 2007).

We have presented the first detection of  $\text{Pa}\beta$  emission for a free-floating object below the deuterium-burning limit. Our analysis of  $\text{Pa}\beta$  and  $\text{H}\alpha$  emission of OTS 44 demonstrates that free-floating objects of a few Jupiter masses can be active accretors. OTS 44 can be seen as free-floating analog of recently detected accreting planetary mass companions that orbit stars (e.g., Bowler et al. 2011, Zhou et al. 2014) and it plays a key role in the study of disk evolution and accretion physics in an extremely low-gravity and -temperature environment.

Furthermore, OTS 44 (M9.5) is the lowest-mass object to date for which the disk mass is determined based on far-IR data. Also interesting in this context is the mm-detection of an M9 dwarf (Scholz et al. 2006). Our detections therefore extend the exploration of disks and accretion during the T Tauri phase down to the planetary mass regime. Plotting the relative disk masses of stars and brown dwarfs including OTS 44 (Fig. .4) shows that the ratio of the disk-to-central-mass of about  $10^{-2}$  found for objects between  $0.03 M_{\odot}$  and  $14 M_{\odot}$  is also valid for OTS 44 at a mass of about  $0.01 M_{\odot}$ . Furthermore, the mass accretion rate of OTS 44 is consistent with a decreasing trend from stars of several solar masses to substellar objects down to  $0.01 M_{\odot}$  (Fig. .5). It is also obvious from this figure that OTS 44 has a relatively high mass accretion rate considering its small mass. These observations show that the processes that accompany canonical star formation, disks and accretion, are present down to a central mass of a few Jupiter masses. This suggests that OTS 44 is formed like a star and that the increasing number of young free-floating planets and ultra-cool T and Y field dwarfs are the low-mass extension of the stellar population.

Figure .6 illustrates how a very young free-floating planetary mass object of about 10 Jupiter masses, such as OTS 44, cools down while aging and becomes an L dwarf at about 10 Myr, similar to PSO J318.5-22, and a Y dwarf at  $\geq 1$  Gyr, similar to WISE 0855-0714. This illustration uses a plot of the evolution of the effective temperature by Burrows et al. (2001). While this might not be the most sophisticated evolutionary model to date and discrepancies with observations can be seen in the temperature (see caption of Fig. .6), it nevertheless shows very nicely the general picture of a substellar object shifting through spectral classes during its evolution.

*Acknowledgements.* We thank K. Luhman for providing the optical spectrum of OTS 44 and the ESO staff at Paranal for executing the SINFONI observations in service mode.

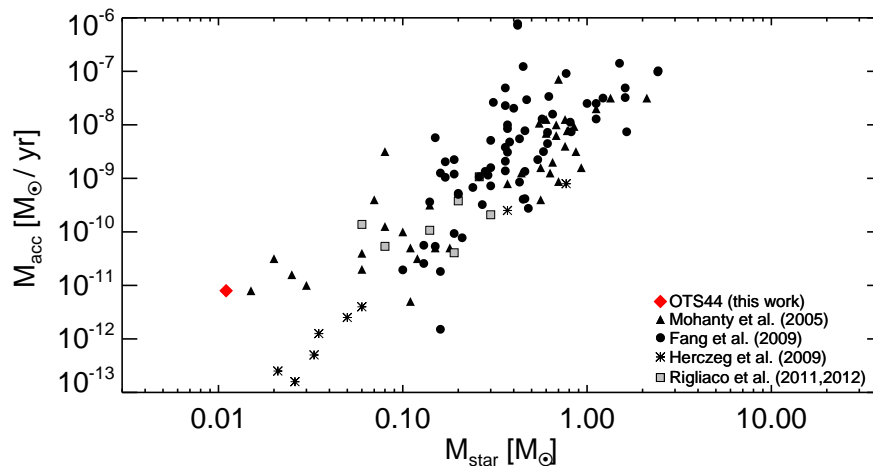


Figure .5: Mass accretion rate versus central mass of stars and brown dwarfs including OTS 44 (red diamond). From Joergens et al. (2013).

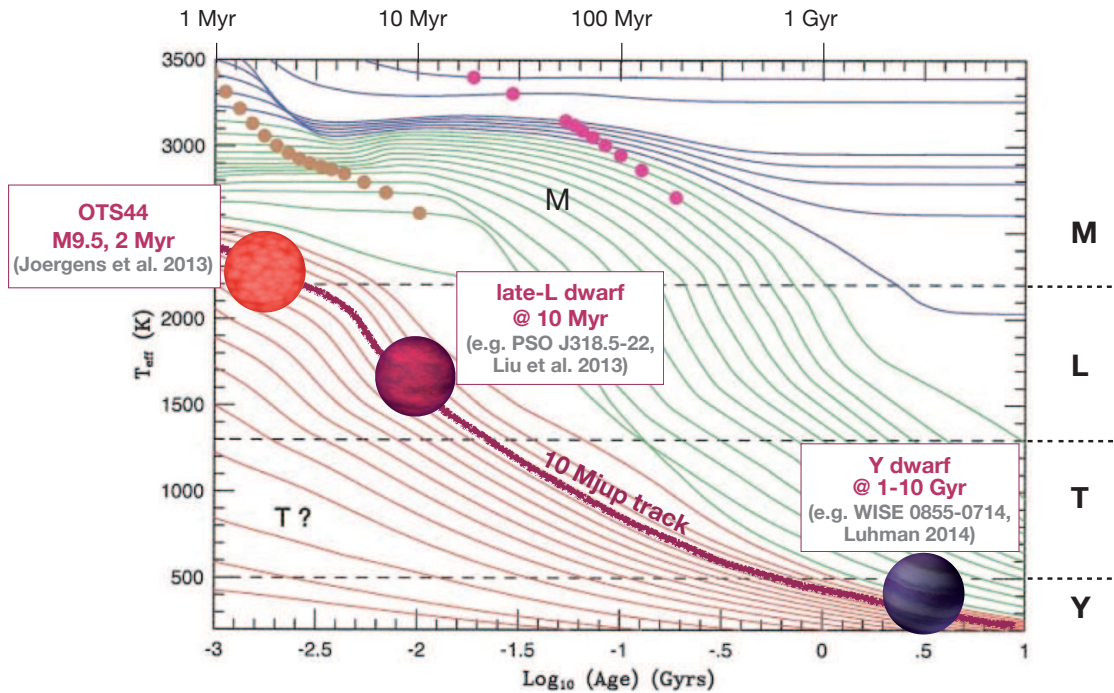


Figure .6: OTS 44 will become a Y dwarf in  $10^9$  years. For this illustration of the evolution of the effective temperature of a very low-mass substellar object we used a plot of Burrows et al. (2001). Note that the model temperatures are hotter than the observationally determined temperatures, which are 1700 K for OTS 44, 1200 K for PSO J318.5-22, and 250 K for WISE 0855-0714.

## References

- Allard, F., Homeier, D., Freytag, B., & Sharp, C. M. 2012, in EAS Publications Series, Vol. 57, ed. C. Reyle, C. Charbonnel, & M. Schultheis, 343
- Bonnefoy, M., Boccaletti, A., Lagrange, A.-M., et al. 2013, A&A, 555, A107
- Bowler, B. P., Liu, M. C., Kraus, A. L., Mann, A. W., & Ireland, M. J. 2011, ApJ, 743, 148
- Burgasser, A. J., Kirkpatrick, J. D., McGovern, M. R., et al. 2004, ApJ, 604, 827
- Burrows, A., Hubbard, W. B., Lunine, J. I., & Liebert, J. 2001, Reviews of Modern Physics, 73, 719
- Cushing, M. C., Kirkpatrick, J. D., Gelino, C. R., et al. 2011, ApJ, 743, 50
- Cushing, M. C., Kirkpatrick, J. D., Gelino, C. R., et al. 2014, AJ, 147, 113
- Delorme, P., Gagné, J., Malo, L., et al. 2012, A&A, 548, A26
- Dupuy, T. J., & Kraus, A. L. 2013, Science, 341, 1492

- Faherty, J. K., Rice, E. L., Cruz, K. L., Mamajek, E. E., & Núñez, A. 2013, *AJ*, 145, 2
- Fang, M., van Boekel, R., Wang, W., et al. 2009, *A&A*, 504, 461
- Harvey, P. M., Henning, T., Liu, Y., et al. 2012, *ApJ*, 755, 67
- Herczeg, G. J., Cruz, K. L., & Hillenbrand, L. A. 2009, *ApJ*, 696, 1589
- Joergens, V., Bonnefoy, M., Liu, Y., et al. 2013, *A&A*, 558, L7
- Joergens, V., Liu, Y., Bayo, A. et al. 2014, in prep.
- Liu, M. C., Magnier, E. A., Deacon, N. R., et al. 2013, *ApJ*, 777, L20
- Luhman, K. L., Peterson, D. E., & Megeath, S. T. 2004, *ApJ*, 617, 565
- Luhman, K. L., Adame, L., D’Alessio, P., et al. 2005, *ApJ*, 635, L93
- Luhman, K. L., D’Alessio, P., Calvet, N., et al. 2005, *ApJ*, 620, L51
- Luhman, K. L. 2007, *ApJS*, 173, 104
- Luhman, K. L., Hernández, J., Downes, J. J., Hartmann, L., & Briceño, C. 2008a, *ApJ*, 688, 362
- Luhman, K. L., Allen, L. E., Allen, P. R., et al. 2008b, *ApJ*, 675, 1375
- Luhman, K. L. 2014, *ApJ*, 786, L18
- Mohanty, S., Jayawardhana, R., & Basri, G. 2005, *ApJ*, 626, 498
- Natta, A., Grinin, V., & Mannings, V. 2000, *Protostars and Planets IV*, 559
- Oasa, Y., Tamura, M., & Sugitani, K. 1999, *ApJ*, 526, 336
- Osterloh, M., & Beckwith, S. V. W. 1995, *ApJ*, 439, 288
- Reipurth, B., & Clarke, C. 2001, *AJ*, 122, 432
- Ricci, L., Testi, L., Natta, A., Scholz, A., & de Gregorio-Monsalvo, I. 2012, *ApJ*, 761, L20
- Ricci, L., Isella, A., Carpenter, J. M., & Testi, L. 2013, *ApJ*, 764, L27
- Rigliaco, E., Natta, A., Randich, S., et al. 2011, *A&A*, 526, L6
- Rigliaco, E., Natta, A., Testi, L., et al. 2012, *A&A*, 548, A56
- Scholz, A., Jayawardhana, R., & Wood, K. 2006, *ApJ*, 645, 1498
- Stamatellos, D., & Whitworth, A. P. 2009, *MNRAS*, 392, 413
- Whitworth, A. P., & Zinnecker, H. 2004, *A&A*, 427, 299
- Wolf, S. 2003, *ApJ*, 582, 859
- Zapatero Osorio, M. R., Béjar, V. J. S., Martín, E. L., et al. 2000, *Science*, 290, 103
- Zhou, Y., Herczeg, G. J., Kraus, A. L., Metchev, S., & Cruz, K. L. 2014, *ApJ*, 783, L17